Int J Adv Manuf Technol (2015) 77:831–838
DOI 10.1007/s00170-014-6491-2

ORIGINAL ARTICLE

Investigating the electrical discharge machining (EDM) parameter effects on Al-Mg_2Si metal matrix composite (MMC) for high material removal rate (MRR) and less EWR–RSM approach

Mehdi Hourmand · Saeed Farahany · Ahmed A. D. Sarhan · Mohd Yusof Noordin

Received: 19 June 2014 / Accepted: 9 October 2014 / Published online: 24 October 2014

Abstract Al-Mg_2Si composite is a new group of metal matrix composites (MMCs). Electrical discharge machining (EDM) is a nonconventional machining process for machining electrically conductive materials regardless of hardness, strength and temperature resistance, complex shapes, fine surface finish/textures and accurate dimensions. A copper electrode and oil-based dielectric fluid mixed with aluminum powder were used. The polarity of electrode was positive. Response surface methodology (RSM) was used to analyze EDM of this composite material. This research illustrates the effect of input variables (voltage, current, pulse ON time, and duty factor) on material removal rate (MRR), electrode wear ratio (EWR), and microstructure changes. The results show that voltage, current, two-level interaction of voltage and current, two-level interaction of current and pulse ON time, and the second-order effect of voltage are the most significant factors on MRR. Pulses ON time and second-order effect of pulse ON time are the most significant factors affecting EWR. Microstructure analysis of EDM on Al-Mg_2Si samples revealed that voltage, current, and pulse ON time have a significant effect on the profile and microstructure of machined surfaced.

Keywords Metal matrix composite (MMC) · Electrical discharge machining (EDM) · Response surface methodology (RSM) · Material removal rate (MRR) · Electrode wear ratio (EWR) · Microstructure

M. Hourmand (✉) · S. Farahany · M. Y. Noordin
Department of Materials, Manufacturing & Industrial Engineering, Faculty of Mechanical Engineering, Universiti Teknologi Malaysia (UTM), 81310 Skudai, Malaysia
e-mail: m.hourmand@gmail.com

A. A. D. Sarhan
Department of Mechanical Engineering, Faculty of Engineering, University of Malaya, 50603 Kuala Lumpur, Malaysia

1 Introduction

Electrical discharge machining (EDM) is a nonconventional machining process that precisely controls sparks falling between the electrode and electrical conductive workpiece causing the removal of material [1–4]. The EDM process is useful for machining electrically conductive materials with various hardness, strength and temperature resistance, complex shapes, fine surface finish/textures, and accurate dimensions [1–3, 5–7]. Adding aluminum powder in the dielectrice leads to increased material removal rate (MRR) and improved surface roughness (SR) during EDM [1, 8]. The chain formation of powder particles in the dielectric helps to bridge the gap between electrode and workpiece which causes the early explosion. Therefore, faster sparking within discharge occurs and faster erosion from the workpiece surface takes place [9]. Al-Mg_2Si composite is a new group of metal matrix composites (MMCs) that could be a better substitute for Al-SiC and Al-Si composites in the aerospace and automotive industries [10, 11] due to their excellent castability, low density, and good wear resistance and mechanical properties [11, 12]. In addition, Al-Mg_2Si composite exhibits potential to be used in the fabrication of automobile brake discs, pistons, piston rings, linear cylinders, and connecting rods because Mg_2Si has a high melting point [13].

Recently, several research works related to the various aspects of EDM on MMCs have been done. It is noted that the Lexicographic Goal Programming (LGP) technique has been selected for optimizing MRR, SR, and recast layers during EDM of Al-6061 composite [6]. Seo et al. [14] chose a copper electrode for the EDM process of 15–35 vol% SiC_p/Al composites. Sidhu et al. [15] explored the effect of PMEDM input variables on the surface modification of three kinds of MMCs (65 vol% SiC/A356.2, 10 vol% SiC-5 vol% quartz/Al, and 30 vol% SiC/A359) using the Taguchi method. Gopalakannan and Senthilvelan investigated about the EDM parameter effect on metal matrix

Table 1 Chemical composition of fabricated composite ingot

Element	Si	Fe	Cu	Mn	Mg	Cr	Ni	Zn	Ti	Al
Wt%	7.07	0.64	2.034	0.217	12.710	0.034	0.003	0.614	0.001	Bal.

nanocomposite (MMNC) of Al-7075 reinforced with 0.5 wt% SiC nanoparticles by applying response surface methodology (RSM) [16]. The effect of input variables during EDM on matrix Al-7075 nanocomposite reinforced with 0.5 wt% B_4C nanoparticles by RSM was studied [17]. Kumar et al. [18] noted that RSM is a method of evaluating EDM parameters on Al-based hybrid MMC (Al-6063/SiC/Al_2O_3/g). Singh and Yeh [19] evaluated EDM parameters on 6061 Al/Al_2O_{3p}/20p aluminum matrix composites (AMCs) for multiple responses using the Taguchi method. Senthilkumar and Omprakash stated that Al-MMCs with 5 and 2.5 % TiC reinforcement using a copper electrode and L18 orthogonal array are suitable conditions for determining the effect of EDM parameters. Velmurugan [20]reported that a central composite rotatable design is one means of evaluating input variables during EDM of Al-6061 hybrid MMCs with 10 % SiC and 4 % graphite particles. EDM of hybrid Al-5%SiC-5 % B_4C and Al-5%SiC-5%Glass MMCs with a copper electrode and L9 orthogonal array has been investigated [21]. As mentioned previously, several researchers have evaluated EDM performance using the RSM and Taguchi methods. Agarwal et al. [22] compared the results of optimizing power consumption after analysis with face-centered central composite design (RSM) and L_{27} orthogonal array (Taguchi method) during the turning process. The results indicate that RSM evaluates the effect of parameters on response and optimizes them better than the Taguchi method.

Fig. 1 AG40L Sodick electrical discharge machine

After conventional MMCs, Al-Mg_2Si is a novel material. There is no research addressing the effects of EDM parameters (voltage, current, pulse ON time, and duty factor) on Al-Mg_2Si in situ composite. High MRR and low electrode wear ratio (EWR) are important in the roughing step of the EDM process. Therefore, developing a mathematical model and simultaneously evaluating the suitable machining parameters for MRR and EWR using the RSM method during the EDM process of Al-Mg_2Si in situ composite are some of the goals of the current research. Another aim is to observe the effects of EDM parameters on the microstructure and surface of machined surfaces.

2 Experimental details

2.1 Fabrication of workpiece

Commercial Al-11.7Si-2Cu alloy, pure aluminium, and pure magnesium were used to fabricate an Al-20Mg_2Si ingot with chemical composition given in Table 1. The composite ingot was first cut into smaller pieces, cleaned, dried, and melted in a 2-kg-capacity SiC crucible using an induction furnace. After around 5 min of allowing homogenization, the melt was stirred, skimmed, and then poured at a temperature of 750± 5 °C into a mild steel mould to fabricate the workpiece with 100×30×200 mm dimensions.

2.2 Experimental conditions and procedure

In this research, the experiments were performed on an AG40L Sodick electrical discharge machine (Fig. 1). A copper electrode with a 5.5-mm diameter was selected. The depth of holes on Al-Mg_2Si in situ composite was 6 mm. The polarity of the electrode was positive, and oil-based dielectric fluid mixed with aluminum powder (PGM WHIT 3) was also used. Voltage, current, pulse

Table 2 The levels of machining parameters

Symbol	Parameters	Unit	Level		
			Low	Center	High
A	Voltage (V)	V	50	80	110
B	Current (I_p)	A	3	9	15
C	Pulse ON time (t_{on})	μs	10	105	200
D	Duty factor[a] (D_f)	%	0.25	0.55	0.85

[a] $Duty\,factor = \frac{Pulse\ ON\ time}{Pulse\ ON\ time + Pulse\ OFF\ tim} \times 100(\%)$

Table 3 Experimental design and results

STD	V	I_p	t_{on}	D_f	MRR (g/min)	EWR (%)
1	50	3	10	0.25	0.00642893	2.07512
2	110	3	10	0.25	0.000340654	2.41758
3	50	15	10	0.25	0.0168624	10.1197
4	110	15	10	0.25	0.016706	10.56
5	50	3	200	0.25	0.000960692	0.291314
6	110	3	200	0.25	0.000115659	0.108578
7	50	15	200	0.25	0.057	0.0714456
8	110	15	200	0.25	0.0204439	0.0238607
9	50	3	10	0.85	0.00577697	1.48488
10	110	3	10	0.85	0.000821067	29.6481
11	50	15	10	0.85	0.0113396	4.98426
12	110	15	10	0.85	0.016479	5.31258
13	50	3	200	0.85	0.000620319	0.129166
14	110	3	200	0.85	0.000296006	0.105513
15	50	15	200	0.85	0.0193183	0.0482276
16	110	15	200	0.85	0.0484091	0.0704225
17	80	9	105	0.55	0.0273418	0.10101
18	80	9	105	0.55	0.0228541	0.201562
19	80	9	105	0.55	0.0207664	0.178982
20	50	9	105	0.55	0.0317546	0.049334
21	110	9	105	0.55	0.00273291	0.102067
22	80	3	105	0.55	0.00283169	0.0529521
23	80	15	105	0.55	0.0575487	0.123824
24	80	9	10	0.55	0.0141248	3.67551
25	80	9	200	0.55	0.0222477	0.0487686
26	80	9	105	0.25	0.0129597	0.0503778
27	80	9	105	0.85	0.0262095	0.123609

MRR material removal rate, *EWR* electrode wear ratio

ON time, and duty factor were chosen as the input variables to analyze MRR and EWR simultaneously. Central composite design (CCD) is one of the most popular response surface methodology (RSM) techniques. The experiments were designed by face-centered CCD consisting of 27 runs including 16 (2^4) two-level factorial design points, 3 center points, and 8 axial points. MRR was computed based on the volume of material removed from the workpiece divided by machining time. EWR was calculated based on the percentage of volume of material removed from the electrode divided by the volume of material removed from the workpiece. Workpiece and electrode weights were measured with a precision electronic balance. Its digital weighing scale has a 0.0001-g precision. In the metallographic process to reveal a particular structure, the samples were prepared by standard grinding using 250- to 4,000-grit SiC sandpaper. Then, Struers Silica OPS suspension (0.5 μm) was used for final specimen polishing until a mirror-smooth surface was obtained. The microstructure was examined with a Nikon optical microscope (MIDROPHOT-FXL). Table 2 illustrates the machining parameter levels and symbols.

3 Results and discussion

Table 3 demonstrates the experimental design and results. The experiment outcomes were analyzed with Design-Expert software. Analysis of variance (ANOVA) was conducted to test the significance of the model, individual model terms, and lack of fit. Natural log transformation was performed on the responses for ANOVA validation. If the "Prob>F" value is less than 0.05, it is significant, but if it exceeds 0.1, it is not

Table 4 ANOVA table for MRR after backward elimination regression

Source	Sum of squares	d.f.	Mean square	F value	Prob>F	Status
Model	77.10	9	8.57	50.11	<0.0001	Significant
A-Voltage	5.49	1	5.49	32.11	<0.0001	
B-Current	47.81	1	47.81	279.68	<0.0001	
C-Pulse ON time	0.42	1	0.42	2.45	0.1356	
D-Duty factor	0.10	1	0.10	0.59	0.4524	
AB	4.00	1	4.00	23.42	0.0002	
AD	1.38	1	1.38	8.05	0.0114	
BC	5.36	1	5.36	31.37	<0.0001	
A^2	2.98	1	2.98	17.45	0.0006	
B^2	1.33	1	1.33	7.76	0.0127	
Residual	2.91	17	0.17			
Lack of fit	2.87	15	0.19	9.80	0.0964	Not significant
Pure error	0.039	2	0.019			
Cor total	80.00	26				
R-squared	0.9637	Adj R-squared		0.9444		
Pred R-squared	0.9021	Adeq precision		25.267		

Table 5 ANOVA table for EWR after backward elimination regression

Source	Sum of squares	d.f.	Mean square	*F* value	Prob>*F*	Status
Model	105.90	8	13.24	35.12	<0.0001	Significant
A-Voltage	0.24	1	0.24	0.63	0.4365	
B-Current	0.046	1	0.046	0.12	0.7308	
C-Pulse On time	78.03	1	78.03	207.04	<0.0001	
D-Duty factor	0.13	1	0.13	0.34	0.5663	
AC	1.66	1	1.66	4.42	0.0499	
AD	1.64	1	1.64	4.35	0.0515	
BC	2.94	1	2.94	7.81	0.0120	
C^2	21.21	1	21.21	56.28	<0.0001	
Residual	6.78	18	0.38			
Lack of fit	6.51	16	0.41	2.98	0.2800	Not significant
Pure error	0.27	2	0.14			
Cor total	112.68	26				
R-squared	0.9398	Adj R-squared		0.9130		
Pred R-squared	0.8359	Adeq precision		18.272		

significant. Significant MRR and EWR models are desirable. Depending on the condition, model terms sometimes are significant and not significant when Prob>*F* value is between 0.05 and 0.1. Moreover, the quadratic model was selected for MRR and EWR due to considerable curvature (curvature was significant) following the first ANOVA analysis (consisting of 19 runs including 16 (2^4) two-level factorial design points and 3 center points). After that, eight axial points were added to the experiment.

Tables 4 and 5 illustrate the ANOVA table for MRR and EWR after backward elimination regression was done. In this trial for MRR response, A, B, AB, AD, BC, A^2, and B^2 were significant. Moreover, A, B, AB, BC, and A^2 were the most significant factors. The ANOVA table results for EWR response show that C, AC, AD, BC, and C^2 were significant. In addition, C and C^2 were the most significant factors. Insignificant lack of fit is desirable for MRR and EWR responses. The insignificant terms can be eliminated from the models by backward elimination regression, so a better model can consequently be produced. After backward elimination regression, hierarchical terms lead to adding D and C to the model for MRR owing to the significant main effect of

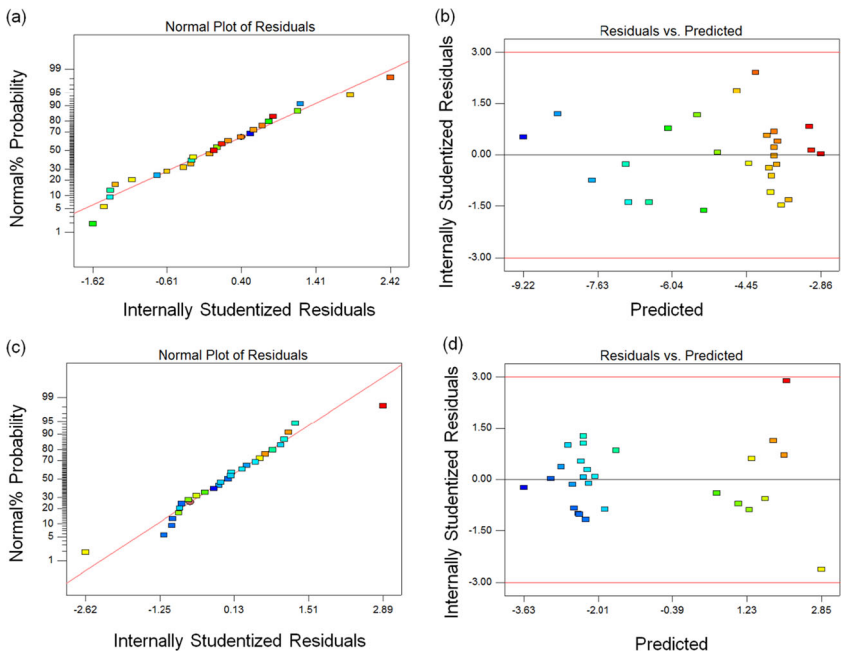

Fig. 2 **a** Normal plot of residuals for MRR. **b** Residuals versus predicted for MRR. **c** Normal plot of residuals for EWR. **d** Residuals versus predicted for EWR

A, AD, B, and BC. Also, A, B, and D were added to the EWR model because C, C^2, AC, AD, and BC were significant.

The outcomes for both MRR and EWR illustrate that an R-squared value which approaches 1 is desirable. In addition, there are minor differences between Adj R-squared and Pred R-squared, meaning that the models have acceptable transaction between the input and output parameters. Adeq precision greater than 4 is desirable, as it measures the signal-to-noise ratio. Therefore, the final regression models in terms of actual factors for MRR and EWR prediction are shown below:

$$\begin{aligned}\mathrm{Ln(MRR)} &= -8.55652 + 0.10685V + 0.25816I_p - 0.010748t_{on} - 2.35626D_f + 0.00277893VI_p + 0.032576VD_f \\ &\quad + 0.00101568I_pt_{on} - 0.00105115V^2 - 0.017527{I_p}^2\end{aligned}$$

$$\begin{aligned}\mathrm{Ln(EWR)} &= +1.78074 - 0.00384356V + 0.070558I_p - 0.049840t_{on} - 2.56403D_f - 0.000113169Vt_{on} \\ &\quad + 0.035573VD_f - 0.000752257I_pt_{on} + 0.000208322{t_{on}}^2\end{aligned}$$

Residuals must be normally distributed with constant variance. Figure 2 shows that a normal probability plot of residuals mapped the residuals versus the predicted response for MRR and EWR after the natural log transformation was applied. Figure 2a, c depicts small departures from the straight line in the normal probability plot of residuals for MRR and EWR, which are common. Figure 2b, d reveals unusual scatter and patterns. Based on these plots, it can be concluded that residuals are normally distributed with constant variance after using the natural log transformation to analyze and model these responses.

Figure 3 illustrates the 3D surface graphs that are curved in conformity with the quadratic models fitted for MRR and

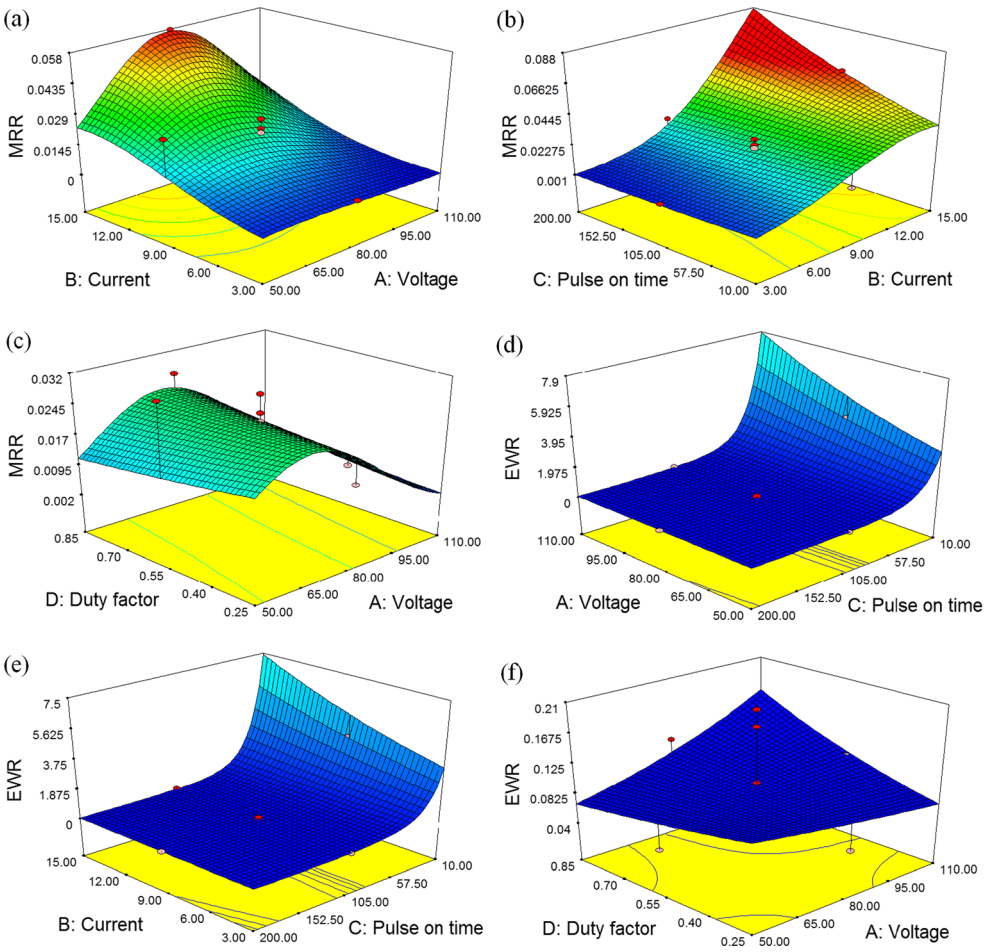

Fig. 3 Response graphs for **a**, **b**, **c** MRR and for **d**, **e**, **f** EWR

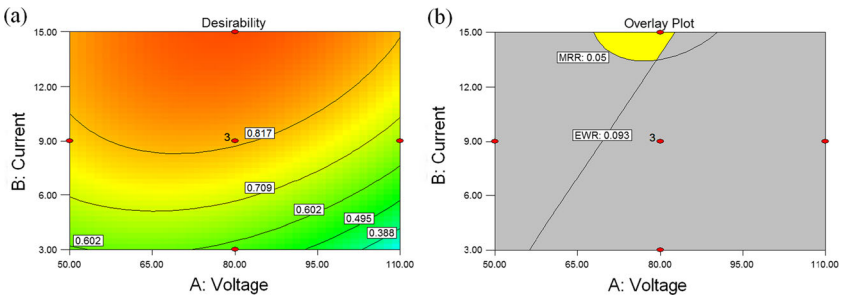

Fig. 4 **a** Desirability graph. **b** Overlay plot

EWR. It is clear from Fig. 3a, b that MRR increases with current amplification because of the rising amount of heat and energy transmitted to the workpiece for melting and vaporization [18]. According to Fig. 3a, c, high MRR is obtainable when the voltage is somewhere in a middle range. The voltage controls the discharge gap between electrode and workpiece. Increasing the voltage will increase the discharge gap [23]. Suitable voltage according to current, pulse ON time, and duty factor results in improved MRR. When current and pulse ON time are at a high level, MRR improves with amplifying voltage of up to 80 V due to the increase in discharge gap and because the chips and debris can easily be removed from this area. Subsequently, the amount of MRR decreases with voltage greater than 80 V because of the discharge gap that is

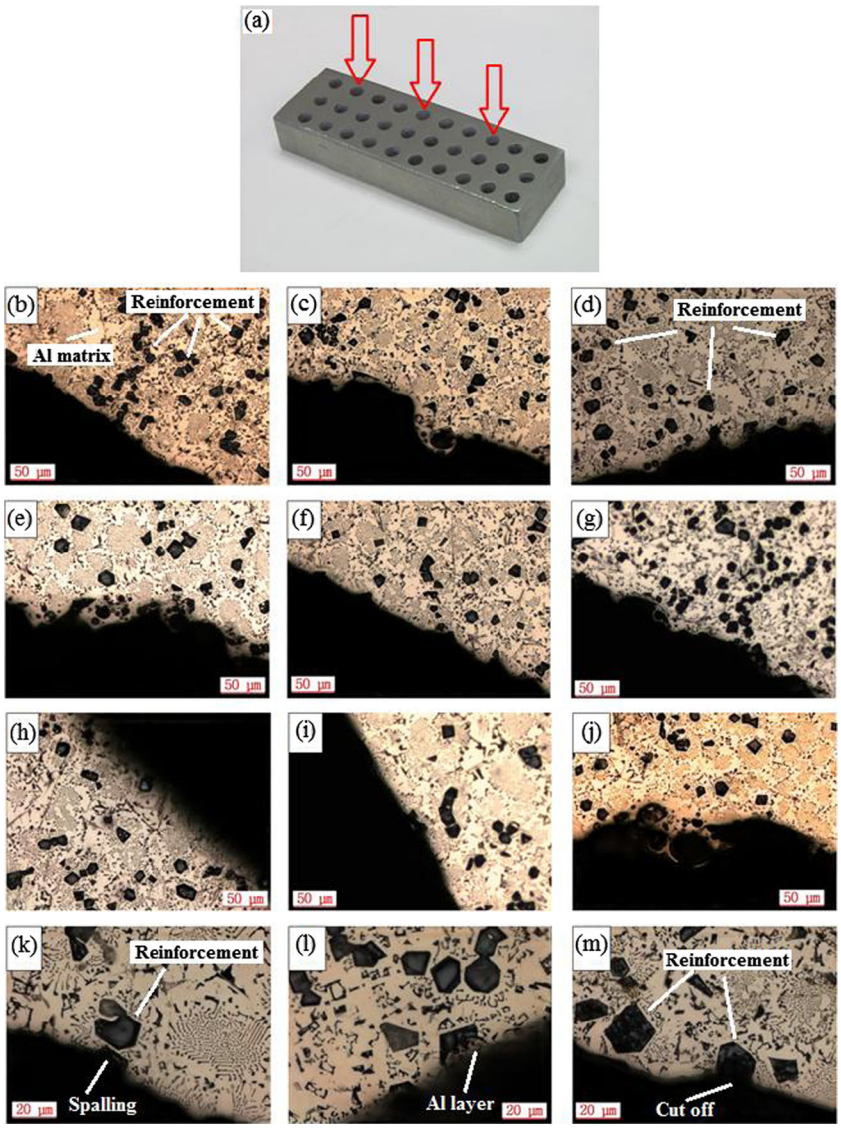

Fig. 5 **a** The image of workpiece and view angle for microstructural analysis. Other images show the cross section of machined surfaces in different voltage, current, pulse ON time, and duty factor. **b** 50 V, 15 A, 10 μs, and 0.25 %; **c** 110 V, 15 A, 10 μs, and 0.25 %; **d** 50 V, 3 A, 200 μs, and 0.25 %; **e** 50 V, 15 A, 200 μs, and 0.25 %; **f** 110 V, 3 A, 10 μs, and 0.25 %; **g** 110 V, 3 A, 200 μs, and 0.25 %; **h** 50 V, 3 A, 10 μs, and 0.25 %; **i** 50 V, 3 A, 10 μs, and 0.85 %; **j** 110 V, 15 A, 200 μs, and 0.85 %; **k** 110 V, 3 A, 10 μs, and 0.25 %; **l** 50 V, 3 A, 200 μs, and 0.25 %; **m** 50 V, 15 A, 10 μs, and 0.25 %

larger than the suitable range [23]. It is obvious in Fig. 3b that by increasing pulse ON time, the trend of MRR improvement is very gradual when the current is at a roughly low level (3 A). However, the highest influence of increasing pulse ON time on MRR occurs when it is combined with the highest current. By increasing pulse ON time, heat energy increases as well, which leads to MRR development [18]. The duty factor, however, has less influence on MRR than other parameters in Fig. 3c.

Figure 3d, e demonstrates that EWR increases with decreasing pulse ON time. Also, the tool wear ratio is at a high level when pulse ON time is at a low level (10 μs). When pulse ON time is quite low with voltage and current amplification, TWR shows an increasingly sharp trend. Figure 3f depicts EWR at a low level when the voltage and duty factor are quite average. Consequently, EWR is low when pulse ON time is approximately more than 80 μs, and the voltage and duty factor are average.

3.1 Desirability, optimization, and conformation

The input variables are adjusted in range. The optimization objective is to discover a condition to simultaneously set maximized and minimized MRR. In the roughing process, increasing MRR is more important than decreasing EWR. So, EWR and MRR are set at 3 pluses (+++) and 5 pluses (+++++) of importance, respectively (in software). When desirability approaches 1, the best setting parameters yield the most desirable responses. The red color depicts the most desirable parameter condition in Fig. 4a. Overlap response on a contour plot represents a feasible region. MRR and EWR were adjusted in the software to more than 0.05 g/min and less than 0.093 %, respectively. The yellow color in Fig. 4b indicates the feasible region for high MRR and low EWR. Two confirmation experiments were performed at two conditions (83 V, 14.5 A, 105 μs, and 0.55 %, and 80 V, 15 A, 200 μs, and 0.55 %). A comparison between predicted and actual values signifies errors of 3.5372 and 6.5634 % for MRR and −1.434 and 1.3752 % for EWR.

3.2 Microstructure

Figure 5a shows the Al-20Mg_2Si MMC workpiece and the view angle for microstructural inspection. Figure 5b, m demonstrates the cross sections of machined surfaces under different conditions. It is evident that EDM parameters have great effect on the microstructure of machined areas but no effect on other regions. Figure 5b, c represents the microstructure of machined surfaces at 50 and 110 V. It appears that increasing voltage produces nonuniform surface and porosity in the machined area due to increasing local energy and discharge gap [23], which leads to some changes in surface roughness. The effect of current on the machined surface is shown in Fig. 5d, e. Surface roughness deteriorates when current changes from 3 to 15 A. In Fig. 5f, g, pulse ON time changes from 10 to 200 μs, leading to the production of a nonuniform surface. The duty factor does not reveal any significant effect on the machined surface profile when it increases from 0.25 to 0.85 % (Fig. 5h, i).

As Fig. 5j shows, the worst profile uniformity was obtained when all parameters were at a high level. On the other hand, three different behaviors were observed in terms of Mg_2Si reinforcement, as seen in Fig. 5k, m. In Fig. 5k, spalling of Mg_2Si particles from the matrix is apparent. Moreover, the aluminum layer covers the Mg_2Si reinforcement (Fig. 5l). In some cases, cutoff particles are observed on the machined surface (Fig. 5m).

4 Conclusion

In this research, Al-Mg_2Si in situ composite underwent EDM with the RSM method. ANOVA analysis for MRR response demonstrated significant voltage, current, two-level interaction of voltage and current, two-level interaction of voltage and duty factor, two-level interaction of current and pulse ON time, second-order effect of voltage, and second-order effect of current. However, voltage, current, two-level interaction of voltage and current, two-level interaction of current and pulse ON time, and the second-order effect of voltage are the most significant factors for MRR. With respect to EWR response, pulses ON time and second-order effect of pulse ON time are the most significant factors. Confirmation test error is less than 6.6 %, which indicates the validation of the predicted models. Microstructure analysis of the EDM process on Al-Mg_2Si samples revealed that voltage, current, and pulse ON time have a significant effect on machined surface profile.

Acknowledgments Sincere regards are to Universiti Teknologi Malaysia (UTM) and University of Malaya Postgraduate Research Grant (PPP) Program No. PG013-2013B.

References

1. Kung K-Y, Horng J-T, Chiang K-T (2009) Material removal rate and electrode wear ratio study on the powder mixed electrical discharge machining of cobalt-bonded tungsten carbide. Int J Adv Manuf Technol 40(1–2):95–104
2. Liu H, Tarng Y (1997) Monitoring of the electrical discharge machining process by abductive networks. Int J Adv Manuf Technol 13(4):264–270
3. Tang L, Guo Y (2014) Electrical discharge precision machining parameters optimization investigation on S-03 special stainless steel. Int J Adv Manuf Technol 70(5–8):1369–1376
4. Teimouri R, Baseri H (2013) Experimental study of rotary magnetic field-assisted dry EDM with ultrasonic vibration of workpiece. Int J Adv Manuf Technol 67(5–8):1371–1384

5. Keskin Y, Halkacı HS, Kizil M (2006) An experimental study for determination of the effects of machining parameters on surface roughness in electrical discharge machining (EDM). Int J Adv Manuf Technol 28(11–12):1118–1121
6. Sidhu SS, Batish A, Kumar S (2013) EDM of metal matrix composite for parameter design using lexicographic goal programming. Mater Manuf Processes 28(4):495–500
7. Yan BH, Wang CC, Liu W, Huang FY (2000) Machining characteristics of Al_2O_3/6061Al composite using rotary EDM with a disklike electrode. Int J Adv Manuf Technol 16(5):322–333
8. Assarzadeh S, Ghoreishi M (2013) A dual response surface-desirability approach to process modeling and optimization of Al_2O_3 powder-mixed electrical discharge machining (PMEDM) parameters. Int J Adv Manuf Technol 64(9–12):1459–1477
9. Garg R, Singh K, Sachdeva A, Sharma VS, Ojha K, Singh S (2010) Review of research work in sinking EDM and WEDM on metal matrix composite materials. Int J Adv Manuf Technol 50(5–8):611–624
10. Jahangiri A, Idris MH, Farahany S (2013) Investigation on tungsten inert gas welding of in situ Al-15 and 20 Mg_2Si composites with an Al-Si filler. J Compos Mater 47(10):1283–1291
11. Zhao Y, Qin Q, Zhao Y, Liang Y, Jiang Q (2004) In situ Mg_2Si/Al–Si composite modified by K_2TiF_6. Mater Lett 58(16):2192–2194
12. Tjong SC, Ma Z (2000) Microstructural and mechanical characteristics of in situ metal matrix composites. Mater Sci Eng R: Reports 29(3):49–113
13. Qin Q, Zhao Y, Xiu K, Zhou W, Liang Y (2005) Microstructure evolution of in situ Mg_2Si/Al-Si-Cu composite in semisolid remelting processing. Mater Sci Eng A 407(1):196–200
14. Seo Y, Kim D, Ramulu M (2006) Electrical discharge machining of functionally graded 15–35 vol.% SiCp/Al composites. Mater Manuf processes 21(5):479–487
15. Sidhu SS, Batish A, Kumar S (2014) Study of surface properties in particulate reinforced MMC using powder-mixed EDM. Mater Manuf processes 29(1):46–52
16. Gopalakannan S, Senthilvelan T (2013) EDM of cast Al/SiC metal matrix nanocomposites by applying response surface method. Int J Adv Manuf Technol 67(1–4):485–493
17. Gopalakannan S, Senthilvelan T (2013) A parametric study of electrical discharge machining process parameters on machining of cast Al/B_4C metal matrix nanocomposites. J Eng Manuf 227(7):993–1004
18. Kumar R, Singh I, Kumar D (2013) Electro discharge drilling of hybrid MMC. Procedia Eng 64:1337–1343
19. Singh S, Yeh M-F (2012) Optimization of abrasive powder mixed EDM of aluminum matrix composites with multiple responses using gray relational analysis. J Mater Eng Perform 21(4):481–491
20. Velmurugan C, Subramanian R, Thirugnanam S, Ananadavel B (2011) Experimental investigations on machining characteristics of Al 6061 hybrid metal matrix composites processed by electrical discharge machining. Int J Eng Sci Technol 3(8):87–101
21. Ahamed AR, Asokan P, Aravindan S (2009) EDM of hybrid Al–SiCp–B_4Cp and Al–SiCp–Glassp MMCs. Int J Adv Manuf Technol 44(5–6):520–528
22. Aggarwal A, Singh H, Kumar P, Singh M (2008) Optimizing power consumption for CNC turned parts using response surface methodology and Taguchi's technique—a comparative analysis. J Mater Process Technol 200(1–3):373–384
23. Egashira K, Matsugasako A, Tsuchiya H, Miyazaki M (2006) Electrical discharge machining with ultralow discharge energy. Precision Eng 30(4):414–420